The pre-equilibrium and equilibrium double differential cross sections for the nucleons and light nuclei induce nuclear reactions on ^{27}Al nuclei

Maha Taha Idrees, Mahdi Hadi Jasim

Department of Physics, College of Science, University of Baghdad, Baghdad, Iraq

E-mail: mahataha9722@yahoo.com

Abstract

The pre - equilibrium and equilibrium double differential cross sections are calculated at different energies using Kalbach Systematic approach in terms of Exciton model with Feshbach, Kerman and Koonin (FKK) statistical theory. The angular distribution of nucleons and light nuclei on ^{27}Al target nuclei, at emission energy in the center of mass system, are considered, using the Multistep Compound (MSC) and Multistep Direct (MSD) reactions. The two-component exciton model with different corrections have been implemented in calculating the particle-hole state density towards calculating the transition rates of the possible reactions and follow up the calculation the differential cross-sections, that include MSC and MSD models. The finite well depth, isospin, shell effects, Pauli effect, charge effect, pairing, surface, angular and linear momentum distributions corrections are considered in this work. The nucleons (n and p) and light nuclei (^{2}D and ^{3}T) have been employed as projectiles at the target ^{27}Al nuclei and at different incident energies (4MeV, 14 MeV and 14.8MeV). The results have been compared with the available experimental and theoretical published work. The comparisons show an acceptable agreement with the TALAYS code (Tendel 2014) for the reactions: ^{27}Al (n, n) ^{27}Al, ^{27}Al (p, n) ^{63}Zn, ^{27}Al (p, D) ^{62}Cu, ^{27}Al (p, p) ^{63}Cu and ^{27}Al (p, ^{4}He)^{60}Ni and at different emission energies and angles.

Key words

Double differential cross sections, pre - equilibrium and equilibrium reactions, FKK model, Exciton model, Kalbach Systematic approach.

Article info.

Received: Apr. 2016
Accepted: May. 2016
Published: Mar. 2017

المقاطع العرضية ثنائية التفاضل لما قبل الاتزان والاتزان للنيكلونات والنوى الخفيفة المحرضة للتفاعلات النووية في النواة ^{27}Al

مها طه أدريس، مهدي هادي جاسم

قسم الفيزياء، كلية العلوم، جامعة بغداد، بغداد، العراق

الخلاصة

تم حساب المقطع العرضي التفاضلي في مرحلة ما قبل الاتزان والاتزان بطاقات مختلفة بواسطة تقريب منهج (كالباخ) مع النظرية الاحصائية لفيشباخ وكيرمن وكونن (Feshbach، Kerman و Koonin (FKK)). تم أعتماد التوزيع الزاوي للنويات والنوى الخفيفة على هدف نواة ^{27}Al، وعند طاقات أنبعاث مختلفة، عند نظام مركز الكتل، أستخدم تفاعلات التركيب والمباشر متعدد الخطوات والمسمات FKK. أنجز نموذج الاكسيتون ثنائي المركبات وعند تصحيحات مختلفة في حساب كثافة المستوى للجسيمة- فجوة، بأتجاه حساب معادلات الانتقال للتفاعلات وتبعها حساب المقاطع العرضية التفاضلية للتفاعلات. اعتمد حساب كثافة المستوي على معلمات التصحيحات التالية: عمق بئر الجهد المحدد، تساوي البرم، تأثير القشرة، تأثير مبدأ باولي، تأثير الشحنة، تأثير الزوج، السطح، توزيعات الزخم الخطي والزاوي. أعتمدت النيكلونات (النيترونات والبروتونات) والنوى الخفيفة كمقذوفات على هدف نواة ^{27}Al وعند طاقات تصادم مختلفة (4MeV,14 MeV 14.8MeV). تم

مقارنة النتائج الحالية مع الاعمال العملية والنظرية المتوفرة في النشريات السابقة. بينت المقارنات توافق مقبول مع شفرة (TALAYS (Tendel 2014 للتفاعلات التالية:
^{27}Al (p, ^{4}He)^{60}Ni و ^{27}Al (n, n) ^{27}Al, ^{27}Al (p, n) ^{63}Zn, ^{27}Al (p, D) ^{62}Cu, ^{27}Al (p, p) ^{63}Cu،
وعند طاقات انبعاث وزوايا مختلفة.

Introduction

Study the mechanism of nuclear reactions is an important task for different areas in nuclear science and engineering, where the measurements of energy spectra and a double differential cross sections of the nucleons (n and p) and light nuclei (^{2}D and ^{3}T) are of great importance that required for the development of fusion reactor materials and ion separation techniques. Since the progress of the pioneering works of [1, 2], the mechanism of nuclear reactions has been characterized into Direct and pre-equilibrium reactions. Follow up this description, different types of reactions and many types of particle emissions are studied and formulated into different successful models as a function of excitation energy, towards building up the satisfaction probability of finding the emitted particle at certain energy channel and angle of emission [3]. Most of the models deal with semi classical approach techniques gathered with Feshbach, Kerman and Koonin (FKK) statistical theory [4], where the considering reactions are included: elastic and inelastic scattering, stripping, knock-out, pick-up, fission and fusion reactions. The pre-equilibrium stage represents the most interested reaction to describe the continuum energy and angular distribution of the expected reaction channel, where the angular momentum distribution (AMD) of the emitted particles is participating in predicting the emitted particles [5-9]. Also, many attempts have been made by [8-11] to include AMD in calculating the emission spectrum. The most comprehensive and successful description of adding AMD was a systematic approach due to [10], where the model based on the parameterization of experimental results and then formulated to include a wide variety of nuclear reactions. Due to reference [4], there are two components of the nuclear reaction: Multi-Step Direct (MSD) component and the Multi-Step Compound (MSC) component. These systematics are known as "Kalbach systematics". A direct and important quantity that can be found using this systematics is the double-differential cross-section, $d^2\sigma/d\Omega d\varepsilon$.

In view of this, and for the necessity enriching the EXFOR national database [11] the (n, p, D, T, ^{3}He and ^{4}He) emission energy spectra and double-differential cross-section at different (n, p, D and T) at different projectile energies (4, 14, 14.8 MeV) with the target nuclei ^{27}Al, have been carefully calculated in the present work using the exciton model associated with FKK model. The results are then compared to the total cross- sections and double-differential cross-section with the available experimental results and theoretical data.

Theoretical model

In this work the pre-equilibrium and equilibrium spectra in terms of Exciton model are calculated and evaluated. These calculations could provide data along the cluster emission preformation probabilities in compound nucleus, when the nuclear reaction mechanism comprises the bridge between fast, direct processes, and accounts for the high-energy tails in emission spectra, and the smooth forward-peaked angular distributions [12-14]. Also, the statistical theory of

FKK [15-17] has been implemented to describe these mechanisms with Exciton model and have been applied in estimating the energy spectrum of nucleons (n and p) and light nuclei (D and T) induced nuclear reactions with ^{27}Al nuclei target [18-20]. At certain reaction and the energy spectrum is one of the quantities that are measured experimentally during nuclear reactions; therefore, the present calculation could be evaluated through comparing with the available published experimental spectra and may be indicate the validity of the present model.

In the present work, the two components primary pre equilibrium (PE) energy spectrum ($d\sigma_{E_b}^{PE}$), for the reaction A(a,b)B, in the framework of the Exciton model via FKK statistical model, for emission of a particle b with emission energy E_b, can be expressed in terms of lifetimes τ for various configurations of states [21] are:

$$d\sigma_{E_b}^{PE} = \sigma_{CF} \sum_{p_\pi=p_\pi^0}^{p_\pi^{max}} \sum_{p_\nu=p_\nu^0}^{p_\nu^{max}} W_b(p_{\pi,\nu}, h_{\pi,\nu}, E_b)\, \tau(p_{\pi,\nu}, h_{\pi,\nu}) \times P(p_{\pi,\nu}, h_{\pi,\nu}) \quad (1)$$

where σ_{CF} is the composite nucleus formation cross-section, $\sigma_{CF=}\ \sigma_{reaction} - \sigma_{direct}$, $\sigma_{reaction}$ is the reaction cross-section derived the optical model theorem and σ_{direct} is the direct cross-section, P is the part of the PE population that has survived the emission b particle and W_b is the emission rate. W_b can be expressed from the pioneer work of [22] as:

$$W_b(p_{\pi,\nu}, h_{\pi,\nu}, E_b) = \frac{2s_b+1}{\pi^2 h^3} \mu_b\ E_b\ \sigma_b^{inv}(E_b)\, \frac{\omega(p_{\pi-Z_b}, p_{\nu-N_b}, h_{\pi,\nu}, E_{tot} - E_b)}{\omega(p_{\pi,\nu}, h_{\pi,\nu}, E_{tot})} \quad (2)$$

where σ_b^{inv} the inverse reaction cross section, which again can be calculated using the optical model theorem, Z_b (N_b) is the proton (neutron) number of the ejectile, E_{tot} is the total energy of the composite system (A*), μ_b is the relative mass of b emission particle and ω is the non equidistant space model (NESM) particle-hole state density, where the total energy and step function are corrected for the threshold energy, finite well depth, isospin, shell effects, Pauli effect, charge effect, pairing, surface, angular and linear momentum distributions corrections and the final equation of the state density is:

$$\omega_b(p_{\pi,\nu}, h_{\pi,\nu}, E_{tot}, T, \Pi) = 0.5 \frac{g_{\pi,\nu}^{p_{\pi,\nu}, h_{\pi,\nu}}(p,h)}{\pi^2 h^3} \times$$

$$\sum_{i_{\pi,\nu}, j_{\pi,\nu}=0}^{p_{\pi,\nu}, h_{\pi,\nu}} (-1)^{i_{\pi,\nu}, j_{\pi,\nu}}\ C_{p_{\pi,\nu}, h_{\pi,\nu}}^{i_{\pi,\nu}, j_{\pi,\nu}} (E_{tot} - \chi)^{n-1}\ \Theta(\chi')\, R(n, E_{tot}, J) f_{iso}(p_{\pi,\nu}, h_{\pi,\nu}, T, T_z) \quad (3)$$

where $C_{p_{\pi,\nu}, h_{\pi,\nu}}^{i_{\pi,\nu}, j_{\pi,\nu}}$ Numerical coefficients, R is the angular momentum distribution function, χ and χ' are the correction factors for the total energy (E_{tot}) and the step function respectively,

$$\chi = (A_k(p_\pi, h_\pi, p_\nu, h_\nu) + S + i_\pi B_\pi + i_\nu B_\nu + j_\pi F_\pi + j_\nu F_\nu) \quad (4)$$

$$\chi' = (E - E_{thresh} - S - i_\pi B_\pi - i_\nu B_\nu - j_\pi F_\pi - j_\nu F_\nu) \quad (5)$$

Also, due to possibility emitted cluster particles in the nuclear reactions, the most dominant probability form of the Nucleon transfer (NT) mechanism must be considered in the present calculations. This mechanism includes the direct pickup or stripping up to three nucleons. It also includes nucleon exchange reactions for inelastic scattering of all light projectiles and for the (t, ^{4}He) and (^{4}He, t) charge exchange reaction. For the reaction ^{27}Al(a,b)Y, the general formula for the NT energy differential cross section is given by [23]:

$$\left[\frac{d\sigma_{a,b}(\varepsilon)}{d\varepsilon}\right]_{NT} = \frac{2s_b+1}{2s_a+1}\frac{A_b}{A_a}\varepsilon\sigma_b(\varepsilon)K_{\alpha,p}\left(\frac{A_a}{E_a+V_a}\right)^{2n}\left(\frac{C_a}{A_B}\right)^{n} \times N_a \sum_{p_\pi}\left(\frac{2Z_A}{A_A}\right)^{2(Z_a+2)h_\pi+2p_\upsilon} \omega_{NT}(p_{\pi,\nu}, h_{\pi,\nu}, U) \quad (6)$$

where

$$\omega_{NT}(p_{\pi,\nu},h_{\pi,\nu},U)=\sum_{i=0}^{3}\sum_{j=0}^{3-i}(X_{NT})^{i+j}\omega(p_\pi+i,h_\pi+i,p_\upsilon+j,h_\upsilon+j,U),$$

the factor X_{NT} is the probability of exciting each additional pair (particle, hole) and it is given by empirical formula given in [24], E_a is the incident energy in the laboratory system, V_a is the average potential drop seen by the projectile between infinity and the Fermi level, C_a and N_a are the normalization constants [23, 25, 26], $K_{\alpha,p}$ is an enhancement factor for (α, N) and (N, α) reactions.

For a complete description of particle emission in a nuclear reaction, another reaction mechanism, such as the knockout process, needs to be considered in addition to exciton model pre-equilibrium emission [27]. Since this model can be used for all projectile types (incident nucleons, α-particles, deuterons, tritons and ^{3}He), the projectile will excite a proton, neutron or α −cluster in the target, and the resulting particles in the composite nucleus can be emitted. The excitation of a nucleon pair by a nucleon projectile is considered in the exciton model, so only the excitation of α −particle is considered here for incident protons and neutrons (p, α) or (n, α). The energy spectrum for the knockout reactions has the form [27]:

$$\left[\frac{d\sigma}{d\varepsilon}\right]_{KO} = \frac{\sigma_a(\varepsilon_a)}{14}(2s_b+1)A_b\varepsilon\,\sigma_b(\varepsilon)\frac{\mathcal{P}_b g_a g_b[U - A_{KO}(p_a, h_b)]}{\sum_{c=a,b}(2s_c+1)A_c\langle\sigma_c\rangle(\varepsilon_m + 2B_{coul,c})} \times \frac{1}{(\varepsilon_m - B_{coul,c})^2 g_a g_b^2/6g_c} \quad (7)$$

where $\mathcal{P}_b$ is the probability of exciting a b-type of particle-hole pair. $B_{coul,c}$ is the Coulomb barrier for a particle of type c. The quantity $\sigma_a(\varepsilon_a)$ is the total reaction cross section for modelling the complex nucleus evaluated at the incident energy, $\langle\sigma_c\rangle$ is the reaction cross section, where a particle of type c is emitted, and averaged over emission energy from $B_{coul,c}$ to the maximum allowed. A_{KO} is the energy independent Pauli correction function.

For knockout reactions the final state consists of an a-type particle and b-type hole, the Pauli correction becomes [27]:

$$A_{KO}(p_a, h_b) = \frac{1}{2g_a} + \frac{1}{2g_b} \quad (8)$$

where g_a, and $g_{b,}$ are the single particle state densities for clusters degrees of freedom of an a-type particle and b-type hole. Generally, the exciton model from its beginnings was designed to describe the energy spectra of the emitted particles, these models ignore the influence of angular momentum. In addition, many theoretical attempts to describe pre-equilibrium angular distributions have proven to be of limited usefulness. The angular distribution has been developed in a series of works [23,25,26] here apply to particles emitted during direct nucleon transfer reactions, during inelastic scattering and knockout reactions involving cluster degrees of freedom, during pre-equilibrium emission (both primary and secondary), and during pre-equilibrium emission (both primary and secondary). The original angular distribution formalism divides the cross section into two components, MSD and MSC, following the suggestion of Feshbach [4]. The MSD part is defined as always having at least one unbound particle degree of freedom at each stage of the reaction, while in the MSC part of the system passes through at least one configuration, where all of the particles are bound so that the information about the original projectile's direction is largely lost. The MSD cross section is thus assumed to exhibit forward-peaked angular distributions, while the MSC cross section has angular distributions which are symmetric about 90^o in the center of mass [23].

$$\frac{d^2\sigma}{d\Omega d\varepsilon_b} = \frac{1}{4\pi}\frac{d\sigma}{d\varepsilon_b}\frac{a_{ex}}{\sinh(a_{ex})}\left[\cosh(a_{ex}\cos\theta) + f_{msd}\sinh(a_{ex}\cos\theta)\right] \quad (9)$$

where a_{ex} is the slope parameter associated with the exciton model and its related components. The angle θ is measured in the center-of-mass system [28].

The quantity $f_{MSD}(\varepsilon_b)$ is the fraction of the cross section at the specified emit energy in the FKK model which is multi-step direct and is here replaced by the fraction that is pre-equilibrium. These cross sections are combined to find the fraction of the cross section f_{MSD}, which represent the pre-equilibrium part [23]:

$$f_{MSD}(\varepsilon) = \frac{[d\sigma/d\varepsilon]_{MSD}}{[d\sigma/d\varepsilon]_{MSD}+[d\sigma/d\varepsilon]_{MSC}} \quad (10)$$

where $[d\sigma/d\varepsilon]_{MSD,}$ is the emission spectra pre equilibrium or forward peaked component contains the exciton model pre equilibrium components, both primary and secondary as well as the cross section from nucleon transfer, knockout and inelastic scattering involving cluster degrees of freedom. Whill, $[d\sigma/d\varepsilon]_{MSC}$, is the emission spectra equilibrium or symmetric component includes only the primary and secondary evaporation cross sections.

Results and discussions

Emission spectra

The nucleon emission spectra for $^{27}_{13}Al$, target nuclei and for incident nucleons, and light nuclei (^{2}D and ^{3}T) using the theoretical approach has been calculated in the present work. The two-component particle-hole state density includes all correction

parameters was used in calculating the spectrum at different incident energies. Its follow up calculating the transition rates and then the differential energy spectrum. Not only the pre-equilibrium emission included in the calculations, but also the particle emission in an equilibrium state. It considered the following normalization factors for squared matrix elements[23, 29],

$$\left|M_{ij}\right|^2 = K_{ij}A_a g^{-3}\left(\frac{E}{3A_a}+20.9\right)^{-3} \quad (11)$$

The validity of exist, such reactions depend on binding energy calculation of primary and secondary emission. As calculated values of the BE for each reaction and nuclei target that used in calculating the cross- section for various reaction mechanisms: direct nucleon transfer cross section, knockout or inelastic cross section involving complex particles plus any collective and elastic cross section, primary exciton model pre-equilibrium cross section, secondary pre-equilibrium cross section, primary equilibrium cross section, secondary equilibrium cross section and the total emission spectra, (the sum of contributions from all of the reaction mechanisms).

It's possible to calculate the energy and differential cross section of the particles in the pre compound towards the continuum stage for ^{27}Al nuclei, therefore, the group of particles corresponding to the discrete states of the compound nuclei $[Al]^*$ clearly can be resolved and depends on the projectile's energy (E_a). At E_n=14.1 MeV incident neutrons with ^{27}Al target different mechanisms have been used, Eqs. (6) and (7), in calculating the energy spectrum at different particle and light nuclei emission energies. As shown in Fig. 1, one can distinguish the probability of the pre equilibrium stage, represents by exciton primary emission, clearly dominant for the reactions (b, c, d and e) among other mechanics of interactions, which indicates the range of pre equilibrium stage exits.

As shown in Fig. 2 the calculated energy spectrum as a function of particle and light particle emission energy of (14.6, 40, 54) MeV incident neutron energy have been evaluated and compared with other theoretical results of [30], and the available experimental data from [31-34], for the reactions; ^{27}Al (n, n) ^{27}Al, ^{27}Al (n, p)^{27}Mg, ^{27}Al (n, D)^{26}Mg, ^{27}Al (n, T)^{25}Mg, ^{27}Al (n, ^{4}He)^{24}Na respectively. The most inconsistency appears when the energy increases above ~4MeV for the reactions Fig. 1b, which indicates the necessity, consideration of re-evaluate the reaction strengths using the two component non ESM exciton model. However, when comparing the calculated energy differential cross-sections based on these spectra, better match with experimental and theoretical are found in the reaction ^{27}Al (n, n)^{27}Al and ^{27}Al (n, p)^{27}Mg, Figs. 1a and b, and follow up less match with the rest of other reactions.

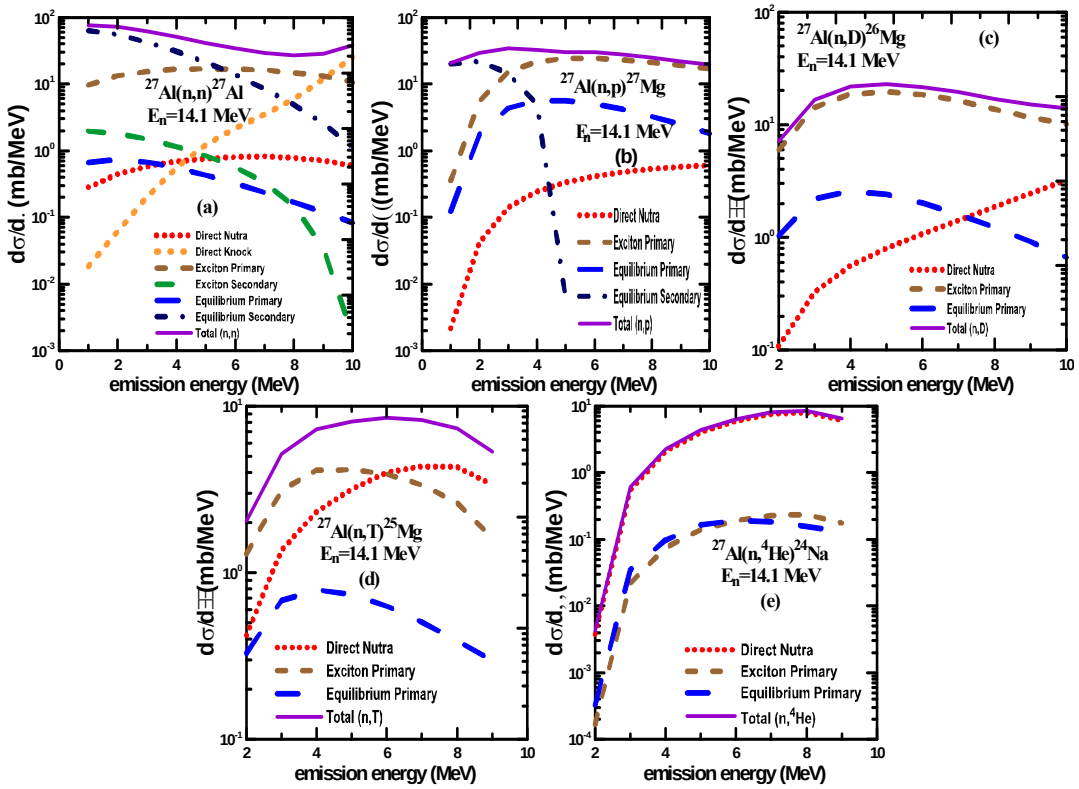

Fig. 1: The energy spectrum of different mechanisms as a function of the particle emission energy in cm-system for emission Nucleons (n and p) and light nuclei (D, T and ^{4}He), for different reactions and at incident energy 14.1MeV, (a) ^{27}Al (n, n) ^{27}Al (b) ^{27}Al (n, p) ^{27}Mg (c) ^{27}Al (n, D) ^{26}Mg (d) ^{27}Al (n, T) ^{25}Mg and (e) ^{27}Al (n, ^{4}He)^{24}Na.

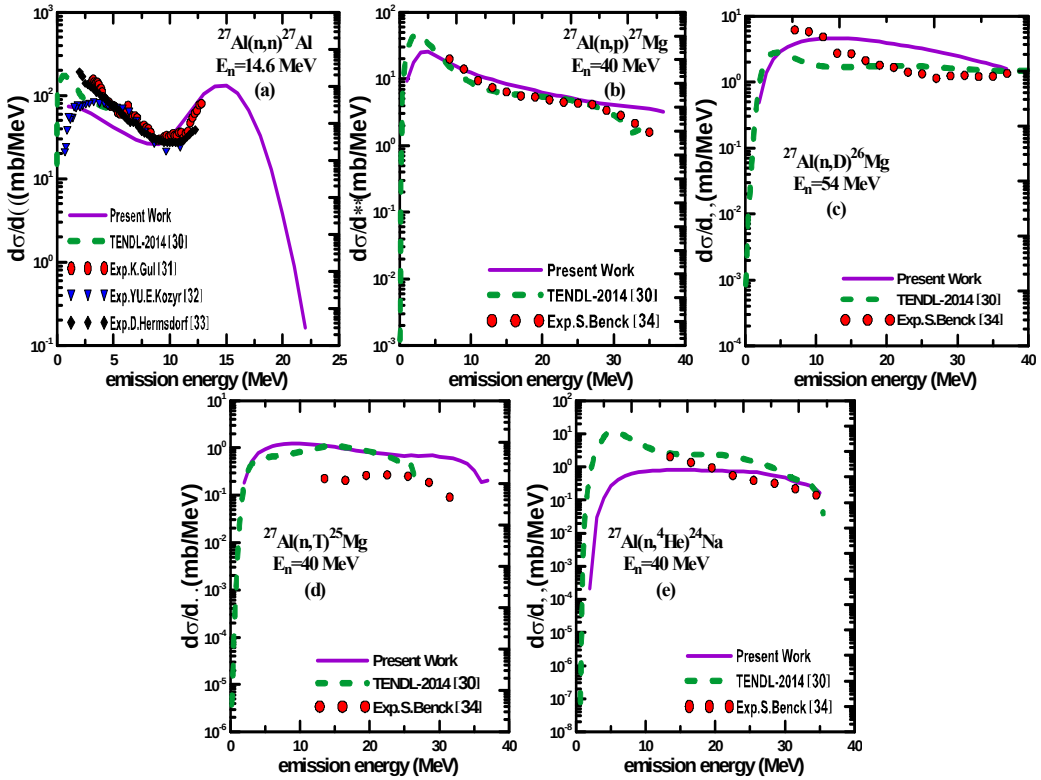

Fig. 2: A comparison between the calculated energy spectrum with refs [30-34], as a function of particle emission energy, at the cm - system, the energy of the incident neutron was (14.6, 40, 54) MeV. (a) ^{27}Al (n, n) ^{27}Al. (b) ^{27}Al (n, p)^{27}Mg (c) ^{27}Al (n, D)^{26}Mg (d) ^{27}Al (n, T)^{25}Mg (e) and ^{27}Al (n, ^{4}He)^{24}Na.

The comparison of the present calculated energy spectrum with others shown in Fig. 3, are in a good agreement with other theoretical results of [30] and the available experimental data from [35, 36], for the reactions; ^{27}Al (p, n) ^{27}Si, ^{27}Al (p, p) ^{27}Al, ^{27}Al (p, D) ^{26}Al, ^{27}Al (p, T) ^{25}Al, ^{27}Al (p, ^{3}He)^{25}Mg, ^{27}Al (p, ^{4}He)^{24}Mg. This indicates the general validity of the present calculations. For ^{27}Al (p, p) ^{27}Al, ^{27}Al (p, D) ^{26}Al, ^{27}Al (p, T) ^{25}Al and ^{27}Al (p, ^{3}He)^{25}Mg reactions, the present results are in excellent agreement with those of other theoretical results and the available experimental data at energy range (5-37) MeV and (20-37) MeV for ^{27}Al (p, ^{4}He)^{24}Mg reactions.

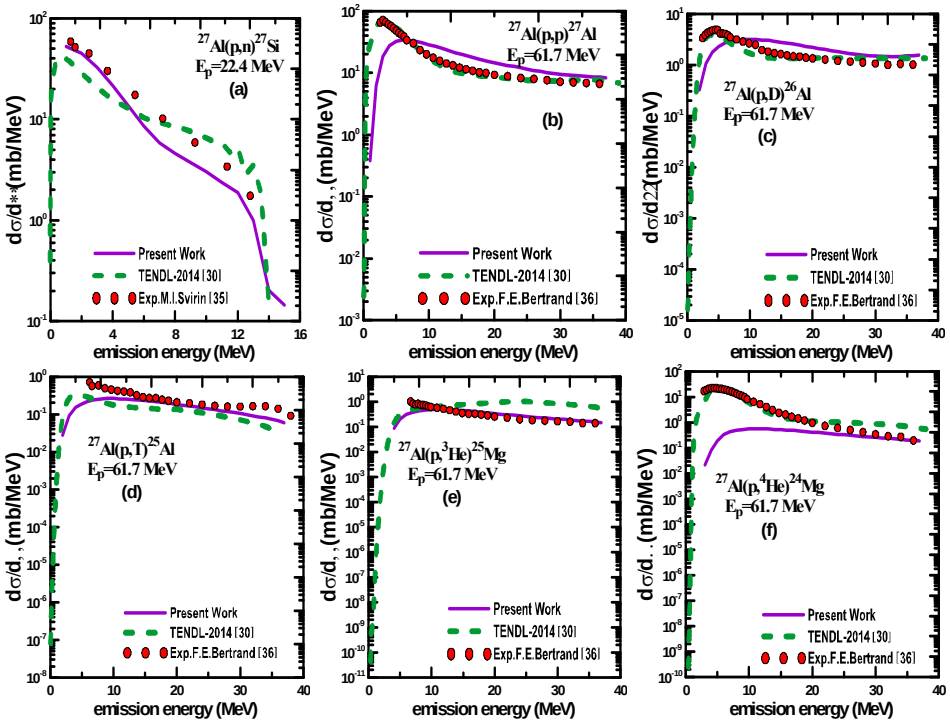

Fig. 3: A comparison between the calculated energy spectrum with refs [30, 35, 36], as a function of particle emission energy in cm-system at 22.4 MeV and 61.7 MeV incident proton for the reactions (a) ^{27}Al (p, n) ^{27}Si (b) ^{27}Al (p, p) ^{27}Al (c) ^{27}Al (p, D) ^{26}Al (d) ^{27}Al (p, T) ^{25}Al (e) ^{27}Al (p, ^{3}He)^{25}Mg (f) ^{27}Al (p, ^{4}He)^{24}Mg.

In Fig. 4, the calculated energy differential cross-sections have been compared with theoretical data of ref [30] for reactions; ^{27}Al (D, n) ^{28}Si, ^{27}Al (D, p) ^{28}Al, ^{27}Al (D, D) ^{27}Al, ^{27}Al (D, T) ^{26}Al, ^{27}Al (D, ^{3}He)^{26}Mg, and ^{27}Al (D, ^{4}He)^{25}Mg and at incident energy 60 MeV. From these comparisons the calculated energy differential cross-sections based on these spectra, better match with theoretical are found in the reactions ^{27}Al (D, T)^{26}Al and ^{27}Al (D, ^{3}He)^{26}Mg, at 60 MeV incident deuterium.

In Fig. 5, when comparing the calculated energy differential cross-sections based on these spectra better match with theoretical of [30] are found in the reactions; ^{27}Al (T, n) ^{29}Si, ^{27}Al (T, p) ^{29}Al, ^{27}Al (T, D) ^{28}Al, ^{27}Al (T, T) ^{27}Al, ^{27}Al (T, ^{3}He)^{27}Mg and ^{27}Al (T, ^{4}He)^{26}Mg. At incident energy 60 MeV. In general, the present results shown in Fig. 5 a good agreement with other theoretical results of [30]. There are no experimental data to compare with the calculated data of ^{27}Al(T,X)Y

reactions. From these comparisons the calculated energy differential cross-sections based on these spectra, better match with theoretical are found in the reactions ^{27}Al (T, ^{4}He) ^{26}Mg, at 60 MeV incident deuterium rather than other channel of reactions.

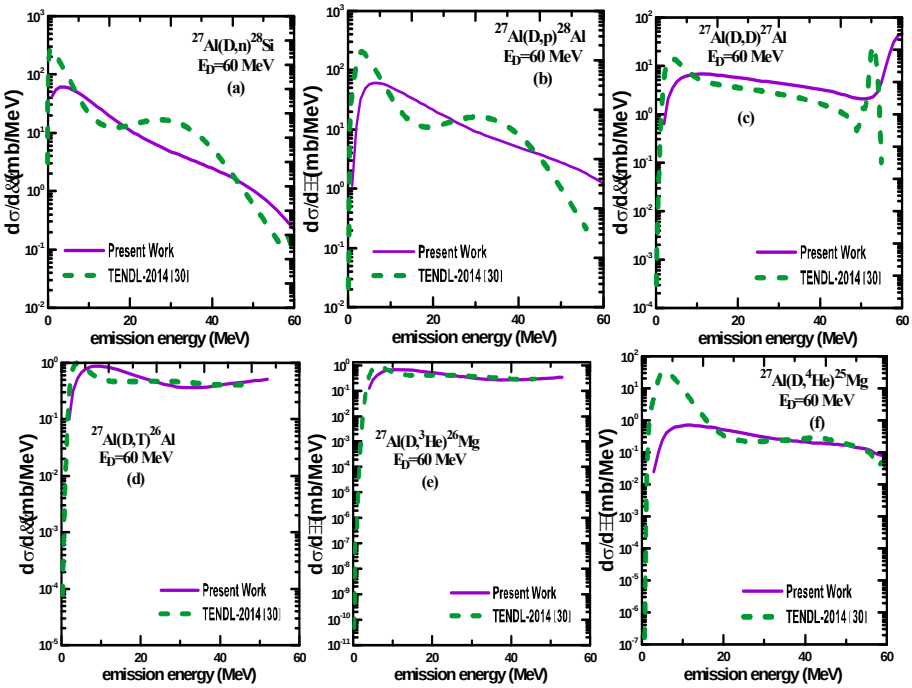

Fig. 4: A comparison between the calculated energy spectrum with refs [30], as a function of particle emission energy in cm-system at 60 MeV incident deuterium for the reactions, (a) ^{27}Al (D, n) ^{28}Si (b) ^{27}Al (D, p) ^{28}Al (c) ^{27}Al (D, D) ^{27}Al (d) ^{27}Al (D, T) ^{26}Al (e) ^{27}Al (D, ^{3}He)^{26}Mg (f) ^{27}Al (D, ^{4}He)^{25}Mg.

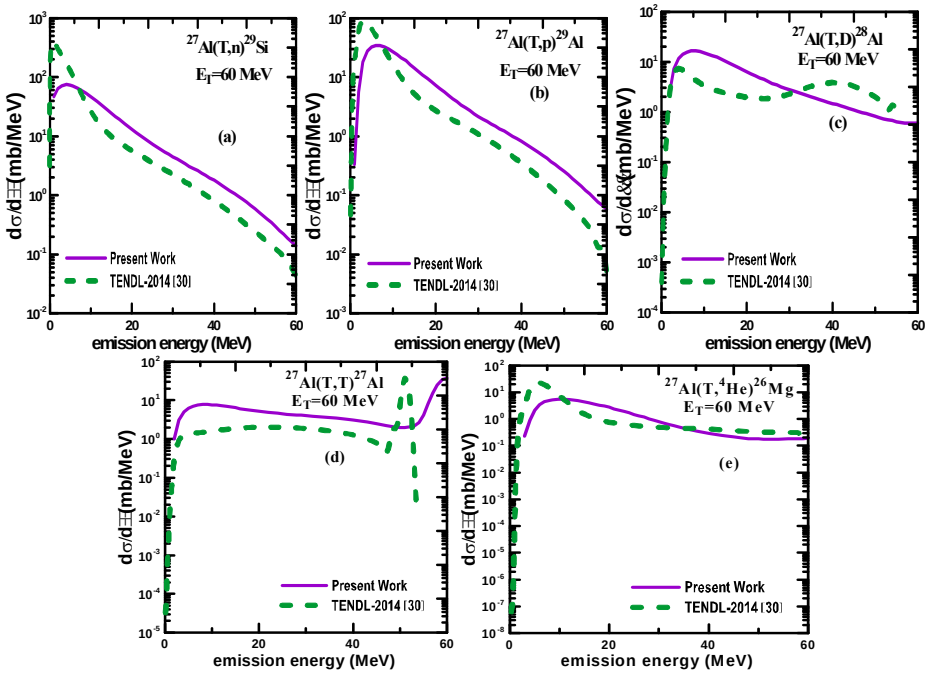

Fig. 5: A comparison between the calculated energy spectrum with refs [30], as a function of particle emission energy in cm-system at 60 MeV incident proton for the reactions, (a) ^{27}Al (T, n) ^{29}Si (b) ^{27}Al (T, p) ^{29}Al (c) ^{27}Al (T, D) ^{28}Al (d) ^{27}Al (T, T) ^{27}Al (e) ^{27}Al (T, ^{3}He)^{27}Mg (f) ^{27}Al (T, ^{4}He)^{26}Mg.

The double differential cross section, DDX

The continuum angular distributions or the double differential cross sections, Eq. (9), for $^{27}_{13}Al$, for incident nucleons (protons and neutrons) and light nuclei (^{2}D and ^{3}T) have been calculated in terms of exciton model and statistical model of FKK, which described in chapter two. The angular distributions are determined by the division of the cross section into its statistical MSD and MSC parts. The main physical parameters determining the shape of the angular distributions, is the energy of the emitted particles and the emission angle, in the center of the mass system.

The dependence of the angular distribution of the emitted energy, and the emission angle is shown in all under figures for emission Nucleons (n and p) and light nuclei (D, T, ^{3}He and ^{4}He), in different reactions. The angular distribution shown in Fig. 6 for incident neutron energy is 14.1 MeV on ^{27}Al the dependence of the angular distribution of the emission energy for different values of emission angle. At emission energies lower than 2 MeV, the value of the emission angle and the incident particle energy does not affect the calculations of the angular distributions. At higher emission energy, the effect of the emission angle is noticed where the smallest emission angle gives the highest angular distribution probability. The largest value of emission is noticed at 14.1 MeV for ^{27}Al target. Also, the energy spectra calculated at 30^0 shows a prominent peak; this peak is less prominent at 30^0, 60^0, 90^0 and 120^0. It is indicated that the neutron emission energy corresponding to the peak is approximately the same as that of the projectile. Since these neutrons have an isotropic distribution in the c.m system, they could be attributed to evaporation from target residues through the equilibrium process. A sudden increase in the angular distribution value is shown in Fig. 6a and at 12.5 MeV emission energy.

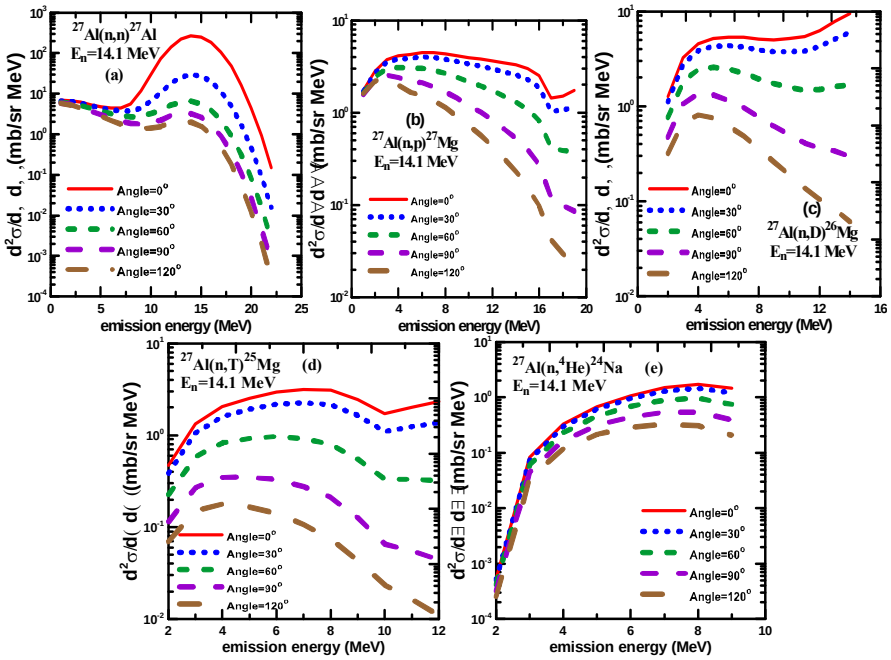

Fig. 6: The double differential cross sections of different mechanisms as a function of particle emission energy in cm-system at 60 MeV incident proton for the reactions, (a) ^{27}Al (n, n) ^{27}Al (b) ^{27}Al (n, p) ^{27}Mg (c) ^{27}Al (n, D) ^{26}Mg (d) ^{27}Al (n, T) ^{25}Mg and (e) ^{27}Al (n, ^{4}He)^{24}Na.

The DDX for neutron induced nuclear reactions with ^{27}Al nuclei at 14.1 MeV incident neutron and emission angles 30^0, 60^0 and 120^0, see Fig. 7a, b, c has been compared with experimental data [36, 39] and other evaluate and theoretical data [30, 37, 38]. It was found an acceptable similarity in the trend in the distribution. Also one can indicate that for slow neutron the main contribution to the DDX spectra comes from the evaporation delivered from CN, while with increasing emission energy the pre-equilibrium stage becomes decisive.

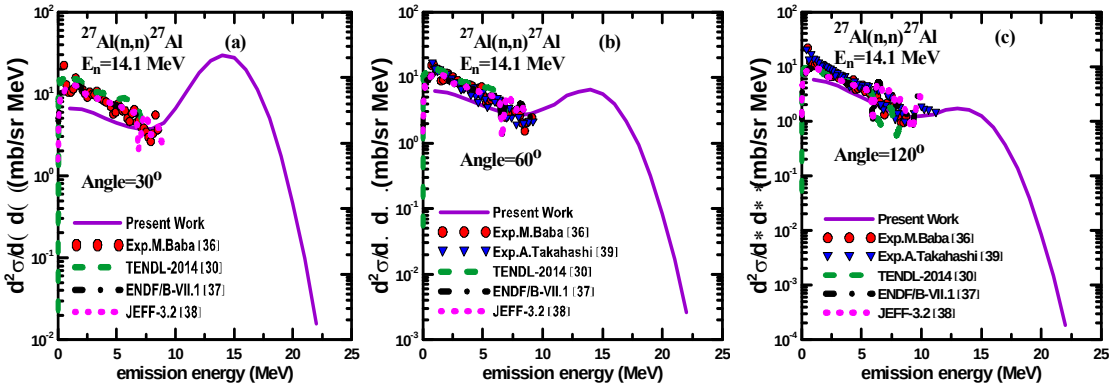

Fig. 7: The double differential cross sections at 14.1 MeV calculated in the present work as a function of emission energy and different emission angle (30^0, 60^0, 120^0) for the reaction ^{27}Al+n and emitted neutron compared experimental data [36, 39] with other theoretical results TENDL [30], ENDF/B-VI [37] and JEFF-3.2 [38].

In Figs. 8 to 12 different angles of emissions (0^0, 30^0,60^0 and 120^0) for nucleon/deuterium induced nuclear reactions with ^{27}Al nuclei are considered (both in the forward and the backward cases) and compared the calculated DDX with the experimental and evaluated data [30, 40, 37, 41-45], for the reactions: ^{27}Al (n,D)^{26}Mg, ^{27}Al(n,T)^{25}Mg, ^{27}Al(p,n)^{27}Si and ^{27}Al(D,n)^{28}Si reaction at neutron energies 28.5 MeV, 34.5 MeV, 39.5MeV, 22 MeV and 22.3MeV respectively. Most of the spectrums shown in the figures are in a good agreement with others, especially at the pre-equilibrium stage of emission energy, where the cross-section depends on emission angle and energy.

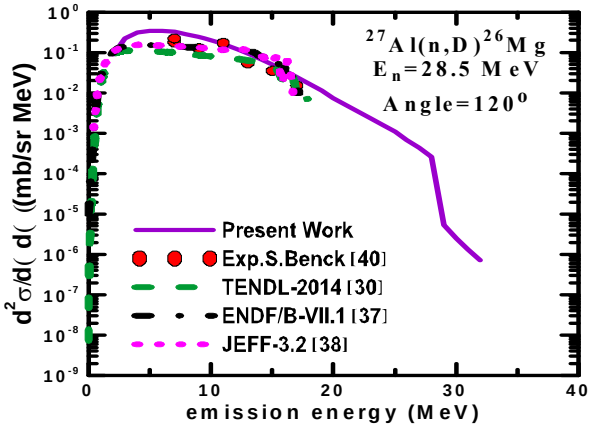

Fig. 8: The double differential cross sections calculated in the present work as a function of emission energy and different emission angle 120^0 for the reaction ^{27}Al+n and emitted deuterium at 28.5 MeV compared with experimental data [40] other theoretical results (TENDL [30], ENDF/B-VI [37] and JEFF-3.2 [38]).

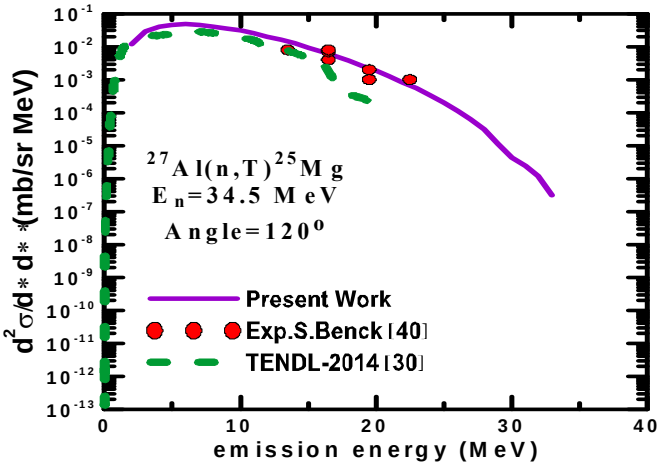

Fig. 9: The double differential cross sections calculated in the present work as a function of emission energy and different emission angle 120^0 for the reaction ^{27}Al+n and emitted triton at 34.5 MeV compared with experimental data [40] other theoretical results TENDL [30].

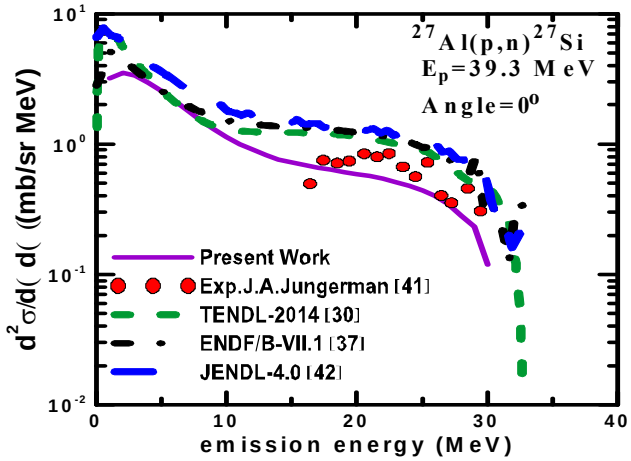

Fig. 10: The double differential cross sections calculated in the present work as a function of emission energy and different emission angle 0^0 for the reaction ^{27}Al+p and emitted triton at 39.3 MeV compared with experimental data [41] other theoretical results (TENDL [30], ENDF/B-VI [37] and JENDL-4.0 [42]).

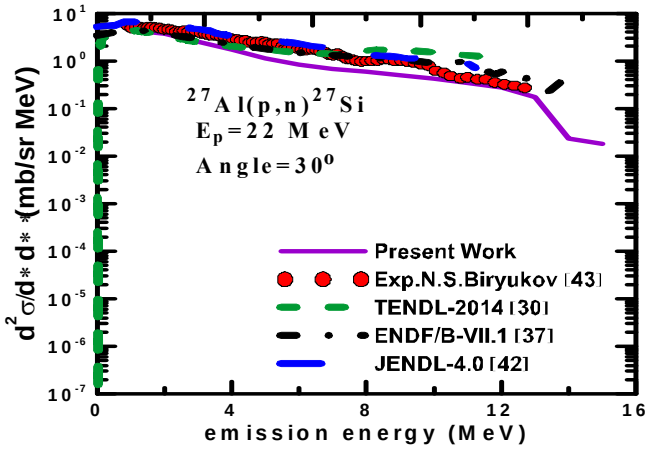

Fig. 11: The double differential cross sections calculated in the present work as a function of emission energy and different emission angle 30^0 for the reaction ^{27}Al+p and emitted triton at 22 MeV compared with experimental data [43] other theoretical results (TENDL [30], ENDF/B-VI [37] and JENDL-4.0 [42]).

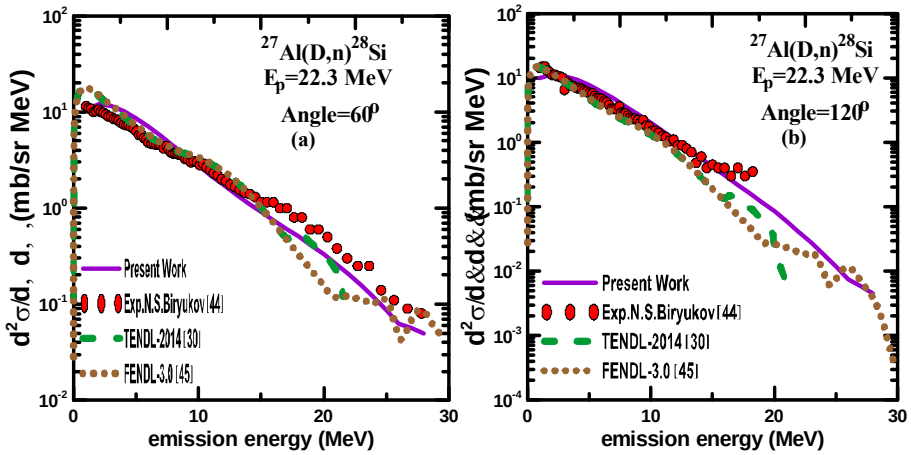

Fig. 12: The double differential cross sections calculated in the present work as a function of emission energy for the reaction ^{27}Al+D and emitted triton at 22.3 MeV compared with experimental data [44] other theoretical results (TENDL [30]] and FENDL-3.0 [45]) and different emission, (a) angle 60^0 and (b) angle 120^0.

Conclusions

The present work focused on a semi classical statistical model (exciton model) with statistical Fashbach, FKK for pre-equilibrium and equilibrium emission calculations. The nucleons and light nuclei (^{2}D and ^{3}T) have been used as a projectile at the target nuclei: $^{27}_{13}Al$, and at different incident energies. Various parameters, reaction considerations and specifications have been taken during the present calculations. The final conclusions made from the results of the present work are:

1- In order to consider a large phenomenological description for the correlated angular and emit energy in the spectrum and for a wide range of possible channels, the two components ESM and NESM total state density used in the present work is included these corrections factors: The finite well depth, isospin, shell effects, Pauli effect, charge effect, pairing, surface, angular and linear momentum distributions corrections are considered in this work.

2- Different mechanisms have been used to calculate the total energy spectrum for the nucleon and light nuclei emission at different incident energies. The exciton model, primary and secondary emission in pre equilibrium and equilibrium stages, and the statistical FKK model, MSD and MSC models for compound formation and direct reactions. These mechanisms improved the comparisons between the present systematic calculations with other experimental and theoretical benchmark data.

3- It was shown indistinguishable calculated results in energy spectrum for the most of the target nuclei of the present work and the results calculated by Talys code, where late one passing the restriction in threshold energy for a particular reaction to be occurring. This also concerns the cluster emission threshold energy which approximately started from zero emission in Talys results for all reactions, while theoretically it is not possible to get a result.

4- The slope parameter is highly affected the results of the angular distributions; this parameter is a function of incident and emission particle energy, e_a and e_b. Through the analysis of the calculated $\frac{d\sigma^2}{d\Omega d\varepsilon}$, data, it is found at low incident energies or one can say below 100 MeV for nucleons (protons or neutrons); the slope parameter, $a_{ex}(e_a, e_b)$, is sensitive to be a function of incident particle's

energy rather than emission energy, while at high incident energies (>100MeV), it is a function of the ratio between the emission and incident energies, and also it shows a transition behavior between these two limits.

References

[1] N. Bohr, Phys. Rev. 54 (1937) 426.
[2] V. Weisskopf, Phys. Rev, 52 (1957) 295.
[3] C. Kalbach, Phys. Rev. C 23 (1981) 124.
[4] H. Feshbach, A. Kerman, S. Koonin, Ann. Phys. (N.Y.) 125, 429 (1980) 476.
[5] J. J. Griffin, Phys. Rev. Lett., 17 (1966) 478-482.
[6] M. Blann, Phys. Rev. Lett., 18, (1968) 1357-1366.
[7] M. Blann, Phys. Rev. Lett. 27, (1971) 337-340.
[8] M. Blann, Phys. Rev. Lett., 28, 12 (1972) 757-759.
[9] M. Blann, Preequilibrium Decay, Ann. Rev. Nucl. Sci. 25, (1975) 123-165.
[10] C. Kalbach and F.M. Mann, Phys. Rev. C. 23 (1981) 112.
[11] V. Mclanc, Rev. EXFOR Basics: A Short Guide to the Nuclear Reaction Data Exchange Format, Brookhaven National Laboratory report BNL-NDC (2000) 63380.
[12] A. I. Dityuk, A. Yu. Konobeyev, V.P. Lunev, Yu. N. Shubin, New Advanced Version of Computer Code ALICE-IPPE INDC (CCP), (1997) 410-452.
[13] A. J. Koning and M. B.Chadwick, Phys. Rev., C. 56, 2 (1997) 970.
[14] E. Gadioli and P.E. Hodgson, Pre-equilibrium Reactions. Clarendon Press. Oxford studies in Nuclear Physics. (1992).
[15] E. A. J. Koning and M.C. Duijvestijn, Nucl. Phys. A744, 15 (2004) 76.
[16] M. B. Chadwick, P. Oblozinsky, P.E. Hodgson, G.Reffo, 2000. IAEA-TECDOC-1178. Phys. Rev, C44, (1991) 814-823.
[17] H. Gruppelaar, P. Nagel, P.E. Hodgson, La Rivista Del Nuovo Cimento, 9 (7) 1 (1986) 46.
[18] R. Bonetti, M. B. Chadwick, P. E. Hodgson, B.V. Carlson, M.S. Hussein, Phys. Rep.202, 4, 171 (1991) 231.
[19] R. Bonetti, A. J. Koning, J. M. Akkermans, P. E. Hodgson, Phys. Rep. 247 (1), 1 (1994) 58.
[20] A. J. Koning, S. Hilaire, S. Goriely, Talys User Manual, A nuclear reaction program, Nuclear Research and Consultancy Group (NRG) Westerduinweg, NL-1755 ZG, Petten, The Netherlands, 2011.
[21] C. Kalbach, Phys. Rev. C 32, (1985) 1157-1187.
[22] C.K. Cline and M. Blann, Nucl. Phys. A172, (1971) 225-276.
[23] C. Kalbach, "User's Manual for PRECO-2006, Exciton Model Pre-equilibrium Nuclear Reaction Code with Direct Reactions", Triangle Universities Nuclear Laboratory, Duke University (February 2007).
[24] J. K. Rasha, The equilibrium and pre-equilibrium D Emission spectra of some nuclei for (n, xD) up to 50MeV. PhD, thesis, Department of Physics, College of Science, University of Baghdad (2011).
[25] S. M. Grimes, R. C. Haight, K. R. Alvar, H. H. Barschall, and R. R. Borchers, Phys. Rev, C 19 (1979) 2127-2137.
[26] A. J. Sprinzak Kennedy, J. C. Pacer, J. Wiley, N. T. Porile, Nuclear Physics, Section A, 203, (1973) 280-330.
[27] C. Kalbach, Phys. Rev. C 71, (2005) 034606, C. Kalbach, Acta Phys. Slov. 45 (1995) 685.
[28] J. P. Meulders, A.Koning, S. Leray, High and Intermediate energy Nuclear Data for Accelerator-driven Systems. HINDAS (2005).
[29] C. Kalbch, Phys. Rev. C 73 (2006) 024614.

[30] A. J. Koning, S. Hilaire, S. Goriely, Talys User Manual, A nuclear reaction program,Nuclear Research and Consultancy Group (NRG) Westerduinweg, NL-1755 ZG, Petten, The Netherlands, TENDL, (2014).
[31] K. Gul, M. Anwar, S. M. Saleem, M. P. Ahmad, Experimental Nuclear Reaction Data, INDC (PAK), 006 (1986).
[32] Yu.E. Kozyr`, G.A. Prokopets, Experimental Nuclear Reaction Data, Yadernaya Fizika 28, 1 (1978) 16.
[33] D. Hermsdorf, A. Meister, S. Sassonoff, D. Seeliger, K. Seidel, Private communication Name. Hermsdorf, Experimental Nuclear Reaction Data, W. HERMSDORF, (1982).
[34] S. Benck, I. Slypen, J. P. Meulders, V. Corcalciuc, M.B. Chadwick, P. G. Young, A. J. Koning, Phys. Rev, C, Nucl. Phys. 58, 3 (1998) 1558.
[35] M. I. Svirin, E. S. Matusevich, S. S. Prokhorov, EXFOR, 6.All-Union Conf. on Neutron Physics, Kiev, 2-6, 3 (1983) 272.
[36] M. Baba, M. Ishikawa, T. Kikuchi, H. Wakabayashi, N. Yabuta, N. Hirakawa,"Experimental Nuclear Reaction Data", C, 88MITO, 209 (1988).
[37] ENDF/B-VII. 1 (Evaluated Nuclear Data File Version B) LANL, ORNL.
[38] JEFF library (Joint Evaluated Fission File and Fusion File), "The JEFF-3.2 Nuclear Data Library".
[39] A. Takahashi, E. Ichimura, Y. Sasaki, H. Sugimoto, "Experimental Nuclear Reaction Data", H. Osaka Univ., OKTAVIAN Reports 87 (1987) 03.
[40] S. Benck, I. Slypen, J. P. Meulders, V. Corcalciuc, M. B. Chadwick, P. G. Young, A. J. Koning, Phys. Rev. C. 58, 3 (1998) 1558.
[41] J. A. Jungerman, F. P. Brady, W. J. Knox, T. Montgomery, M. R. Mcgie, J. L. Romero, Y. Ishizaki, "Experimental Nuclear Reaction Data", J, NIM. 94 (1971) 421.
[42] JENDL-4.0/HE, K.Kosako, SIT. SHIMZ, (2007).
[43] S. Biryukov, B. V. Zhuravlev, A. P. Rudenko, O. A. Salnikov, V. I. Trykova, "Experimental Nuclear Reaction Data", EXFOR,YF, 31, 3 (1980) 561.
[44] N. S. Biryukov, B. V. Zhuravlev, A. P. Rudenko, V. I. Trykova, "Experimental Nuclear Reaction Data", YF, 2 (1986) 6.
[45] FENDL-3.0, library. (Nuclear Data Libraries for Advanced System: Fusion Devices), "The FENDL-3.0 Nuclear Data Library (1965).